ON THE NON-UNIQUENESS OF THE REFRACTION SOLUTION

ORHAN GÜRELI[1] and TURAN KAYIRAN[2]

[1] *ARAR Oil and Gas Inc., Dumluca Sok. 19. 06530 Beysukent, Ankara, Turkey. orhangureli2@yahoo.com.tr*
[2] *Ankara University, Faculty of Engineering, Geophysical Department, 06100 Tandogan, Ankara, Turkey. turankayiran@yahoo.com*

(Received January 20, 2017; revised version accepted November 2, 2017)

ABSTRACT

Güreli, O. and Kayiran, T., 2018. On the non-uniqueness of the refraction solution. *Journal of Seismic Exploration*, 27: 1-27.

The seismic refraction method has long been recognized as an efficient tool for obtaining information on subsurfaces. In this paper, we investigate a dipping refractor case and demonstrate that two sets of solutions exist. The determination of the static (weathering) corrections of seismic surveys is largely based on refraction; such a model may be considered to be specific and of limited interest. However, this model has, in fact, been widely utilized since the early days of seismic surveys. It is known that all relevant refraction analyses used to date yield a unique theoretical solution for the researched parameters. In our paper, through a different approach, we demonstrate that it is possible to express the solution of the refraction problem in terms of a second degree equation and according to the behavior of the discriminant to obtain two sets of solutions. Synthetic and real data examples are presented after the theoretical explanation.

KEY WORDS: refraction, near surface modeling, first break picking, traveltimes, dipping layer, reciprocal method, seismic velocities, single-shot.

INTRODUCTION

The correct estimation and removal of the effects of near-surface weathered layers is an important issue for seismic reflection surveys. To remove these effects we must often characterize the subsurface by geophysical methods. Seismic refraction constitutes one of the most valuable tools for handling static corrections properly for seismic surveys.

0963-0651/18/$5.00

Over the years, the interpretation of refraction data has been a subject of research and several methods have been proposed in this context.

One method commonly used is the intercept method, described by Mota (1954) for the multi-layers case. For a single refractor, this method can be summarized as the solution of two linear equations, represented by two shoots, with two unknowns, represented by the dip and critical angle. The angle of incidence into the refracting bed i_1 and the angle of dip of the refractor θ_1 are given by (A-7) and (A-8) in the Appendix as

$$i_1 = \frac{1}{2}\left[\arcsin\frac{v_o}{v_{1a}} + \arcsin\frac{v_o}{v_{1b}}\right]$$

$$\theta_1 = \frac{1}{2}\left[\arcsin\frac{v_o}{v_{1a}} - \arcsin\frac{v_o}{v_{1b}}\right] \quad ,$$

where v_{1a} and v_{1b} are apparent refractor velocities, and v_o is the first layer's velocity.

Eqs. (A-7) and (A-8) lead to a single solution for i_1 and θ_1, respectively, and, starting from these equations, the velocity and the depth found using Snell's law and intercept time necessarily imply a unique solution.

The second approach is the concept of time delay, which was introduced by Gardner (1939) and used by several authors, such as Barthelmes (1946), Tarrant (1956) and Barry (1967), resulting in a unique, continuous profiling of the refractor, as shown by Telford et al. (1990).

We can say that in this approach, the intercept is replaced by delay time to find the refractor position in the subsurface.

Other refraction interpretation techniques that use geometrical reconstruction methods based on wave fronts constitute the third approach. These techniques commonly use reciprocal time for the reconstruction of the refractor and equally produce a unique representation of the subsurface. Among them, Thornburgh (1930), Hagedoorn (1959), Hales (1958) can be cited.

In addition to these methods for the estimation of the near surface parameters, seismic refraction inversion approaches that use the tomography algorithm should also be mentioned. They are based on the minimization of

the residual between the observed and modeled data using a least squares criterion. Most of them are related to the ray-tracing tomography methods (White, 1989; Doherty, 1992; Shtivelman, 1996; Zhang and Toksöz, 1998; Chang et al., 2002). All of these inversion approaches result in an approximate value for the researched parameter according to the assumption made on the minimization of the residual and have no pretention to attain the absolute value of the unknown through an algebraic expression but are applicable to any arbitrary velocity models.

At this point, it should be noted that it is theoretically possible to reach the non-unique solution of this problem through tomographic inversion. However, in this case, the following remarks should be considered

1. The a priori the inversion process does not predict whether the conditions required for non-uniqueness are satisfied, as we discussed in the paragraph "Discussion on the non-uniqueness of the roots".
2. According to the reference model from which we start iterating, the result may converge to one of the solutions, ignoring the other probable solution even if it exists.
3. To overcome this difficulty and detect two solutions at once, it is possible to introduce the parameters over a very large scale. However, if the non-uniqueness conditions are not satisfied, this extra precaution appears to be useless and wasteful.
4. As we mentioned above, the inversion algorithm gives the approximate values of the unknown parameters tributary of the least squares criterion used for the inversion. In this respect the superiority of the analytical solutions, if it exists, is indisputable.
5. Apart from these methods, second degree in the dip measured from the horizontal for the first refractor interface, we propose an alternate approach, substantially different from the others, that produces a second degree expression for the resolution of the refraction problem.

THEORY

The general assumptions involved for one refractor model are as follows:

1. The refractor, along which the waves travel and return to the surface, is linear.
2. The medium velocities are constant within the subsurface illumination area of the refraction experiment.
3. The sign of dip angle of refractor is taken as positive for the positive trigonometric direction, starting from the horizontal.
4. The recording scheme is as illustrated in Fig. 1.

From Fig. 1, we can write for the $+x$-direction:

$$t_{x1}^{+} = \frac{OA}{v_o} + \frac{AB}{v_1} + \frac{BC}{v_o} = \frac{Z_1}{v_o \cos i_1} + \frac{x\cos\theta_1 - (Z_1 + z_1)}{v_1} \tan i_1 + \frac{z_1}{v_o \cos i_1} \quad , \qquad (1)$$

after simplification, (1) becomes

$$t_{x1}^{+} = \frac{x\cos\theta_1}{v_1} + (Z_1 + z_1)\frac{\sqrt{v_1^2 - v_o^2}}{v_o v_1} \quad ,$$

$$t_{x1}^{+} = \frac{x\cos\theta_1}{v_1} + (Z_1 + Z_1 - x\sin\theta_1)\frac{\sqrt{v_1^2 - v_o^2}}{v_o v_1} \quad ,$$

$$t_{x1}^{+} = \frac{x\cos\theta_1}{v_1} - x\frac{\sqrt{v_1^2 - v_o^2}}{v_o v_1}\sin\theta_1 + \frac{2Z_1\sqrt{v_1^2 - v_o^2}}{v_o v_1} \quad ,$$

$$t_{x1}^{+} = x\left(\frac{\cos\theta_1}{v_1} - \frac{\sqrt{v_1^2 - v_o^2}}{v_o v_1}\sin\theta_1\right) + \frac{2Z_1\sqrt{v_1^2 - v_o^2}}{v_o v_1} \quad , \qquad (2)$$

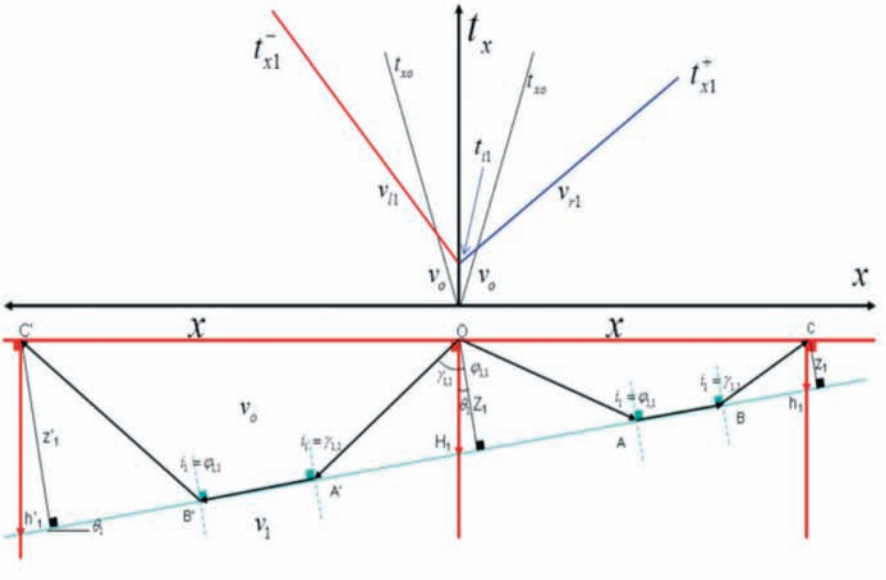

Fig. 1. Split shooting refraction for the two-layer case with dipping interface.

where
v_0: the first layer velocity,
v_1: the second layer velocity,
θ_1: the dip measured from the horizontal for the first refractor interface,
i_1 : critical angle for the first refracting interface,
z_1: the perpendicular depth of the refractor at the receiver point (see Fig 1),
Z_1: the perpendicular depth of the refractor at the shot point.

In a similar way, we find for the $-x$-direction

$$t_{x1}^{-} = x\left(\frac{\cos\theta_1}{v_1} + \frac{\sqrt{v_1^2 - v_o^2}}{v_o v_1}\sin\theta_1\right) + \frac{2Z_1\sqrt{v_1^2 - v_o^2}}{v_o v_1} \quad . \tag{3}$$

These two last equations can be viewed as the expression of two lines as (Fig. 2)

$$t_{x1}^{-} = ax + c \quad , \tag{4}$$

$$t_{x1}^{+} = bx + c \quad , \tag{5}$$

where

$$a = \frac{1}{v_{r1}} = \frac{\cos\theta_1}{v_1} + \frac{\sqrt{v_1^2 - v_o^2}}{v_o v_1}\sin\theta_1 \quad , \tag{6}$$

$$b = \frac{1}{v_{l1}} = \frac{\cos\theta_1}{v_1} - \frac{\sqrt{v_1^2 - v_o^2}}{v_o v_1}\sin\theta_1 \quad , \tag{7}$$

where v_{r1} and v_1 are apparent velocities and

$$c = \frac{2Z_1\sqrt{v_1^2 - v_o^2}}{v_o v_1} \quad , \tag{8}$$

The arithmetic mean of these two equations (Fig. 2) is

$$\frac{t_{x1}^{+} + t_{x1}^{-}}{2} = t_{x1}^{o} = \frac{a+b}{2}x + c = x\frac{\cos\theta_1}{v_1} + c = x\frac{\cos\theta_1}{v_1} + t_{i1} \, , \tag{9}$$

where t_{i1} is the intercept time.

It should be mentioned that, in order to avoid any misunderstanding, the mean value does not imply an approximation.

For the intersection point of the mean line t_{x0} with the line x/v_0, (9) becomes

$$x_c\left(\frac{\cos\theta_1}{v_1}\right)+t_{i1}=\frac{x_c}{v_o} \quad , \tag{10}$$

where x_c is the abscissa of the intersection point. The value of x_c is obtained from (6), (7) and (10) as

$$x_c=\frac{-t_{i1}}{\left[\frac{a+b}{2}-\frac{1}{v_o}\right]}=\frac{-t_{i1}}{\left[\frac{1}{2}\left(\frac{1}{v_{r1}}+\frac{1}{v_{l1}}\right)-\frac{1}{v_o}\right]} \quad , \tag{11}$$

which is a function of apparent velocities, v_{r1},v_{l1} and v_0,t_{i1} and easily calculable.

We are, now, able to determine the value of refractor velocity (v_1). From (10), we can write

$$v_1=\frac{v_o x_c}{\left(x_c-v_o t_{i1}\right)}\cos\theta_1 \quad . \tag{12}$$

On the other hand, by subtracting (7) from (6) we obtain

$$a-b=\left[\frac{\cos\theta_1}{v_1}+\frac{\sqrt{v_1^2-v_o^2}}{v_o v_1}\sin\theta_1\right]-\left[\frac{\cos\theta_1}{v_1}-\frac{\sqrt{v_1^2-v_o^2}}{v_o v_1}\sin\theta_1\right] \quad ,$$

$$a-b=2\sin\theta_1\frac{\sqrt{v_1^2-v_o^2}}{v_o v_1} \quad , \tag{13}$$

solving (13) for v_1 gives

$$v_1=\frac{2v_o\sin\theta_1}{\left(4\sin^2\theta_1-v_o^2(a-b)^2\right)^{1/2}} \quad . \tag{14}$$

Using the equality of (12) with (14) and putting

$$A = \frac{v_o x_c}{\left(x_c - v_o t_{i1}\right)} \quad , \tag{15}$$

$$B = \frac{v_o^2 \left(a-b\right)^2}{4} \quad , \tag{16}$$

we can write

$$A\cos\theta_1 = \frac{2v_o \sin\theta_1}{\left(4\sin^2\theta_1 - v_o^2\left(a-b\right)^2\right)^{1/2}} \quad , \tag{17}$$

$$A^2 - \frac{A^2 B}{\sin^2\theta_1} - A^2 \sin^2\theta_1 + A^2 B = v_o^2 \quad , \tag{18}$$

with

$$\sin^2\theta_1 = y \quad , \tag{19}$$

(18) becomes

$$A^2 - \frac{A^2 B}{y} - A^2 y + A^2 B = v_o^2 \quad . \tag{20}$$

Rearranging (20) with respect to *y* yields

$$y^2 + \left[\frac{v_o^2}{A^2} - 1 - B\right] y + B = 0 \quad , \tag{21}$$

which is an equation of the second order for *y*.

Solving (21) for *y*, two roots

$$y_1 = \frac{-\left[\frac{v_o^2}{A^2} - 1 - B\right] - \sqrt{\Delta}}{2} \quad , \tag{22}$$

and

$$y_2 = \frac{-\left[\frac{v_o^2}{A^2} - 1 - B\right] + \sqrt{\Delta}}{2} \quad , \tag{23}$$

are obtained.

Where Δ is the discriminant of eq. (21).

$$\Delta = \left[\frac{v_o^2}{A^2} - 1 - B\right]^2 - 4B \quad . \tag{24}$$

Combining these two values of y with (19) yields

$$\sin\theta_1 = \mp\sqrt{y_1} \quad , \tag{25a}$$

$$\sin\theta_1' = \mp\sqrt{y_2} \quad . \tag{25b}$$

Using the equality of (8)

$$Z_1 = \frac{v_o v_1 t_{i1}}{2\sqrt{v_1^2 - v_o^2}} \quad , \tag{26}$$

is obtained. From Fig. 1, we can write

$$H_1 = Z_1 / \cos\theta_1 \quad , \tag{27}$$

where H is the vertical depth beneath the shot point for the first refracting interface.

The sign of the square root is determined by comparing two time values t_{OABC} and $t_{OA'B'C'}$ (Fig. 1). If t_{OABC} *is* smaller than $t_{OA'B'C'}$, the plus sign should be considered. Otherwise, the minus sign is to be taken.

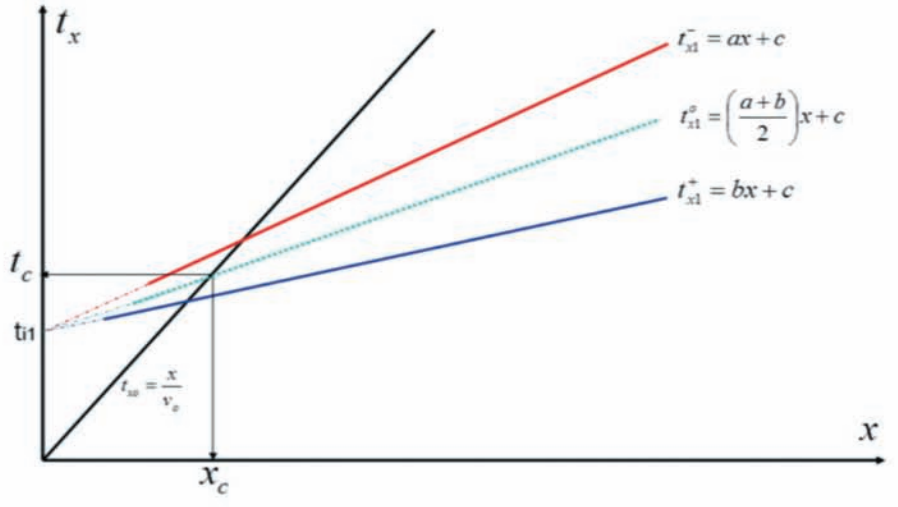

Fig. 2. Mean value t_{x1}^o of two t_{x1}^+ and t_{x1}^- lines.

Theoretically, two relevant y_1 and y_2 values honor the time-distance expression. In other words, for the same intercept, v_0, v_{r1} and v_{l1} it is possible to obtain two sets of solutions of v_1, θ_1 and H_1 for the subsurface. This result contradicts the existence of a unique theoretical solution given by the conventional methods mentioned above (Fig. 3). Intersection points of the graphs represented by eqs. (12) and (14) give a set of solution for v_1 and θ_1. These two approaches necessarily yield the same results because they start from the same equations. We provide a numerical proof of these results using examples with synthetic and real data applications.

DISCUSSION ON THE NON-UNIQUENESS OF THE ROOTS

We start from formula (24) which is the discriminant of the second degree eq. (23).

$$\Delta = \left[\frac{v_o^2}{A^2} - 1 - B\right]^2 - 4B \quad .$$

In order to get one root, the condition

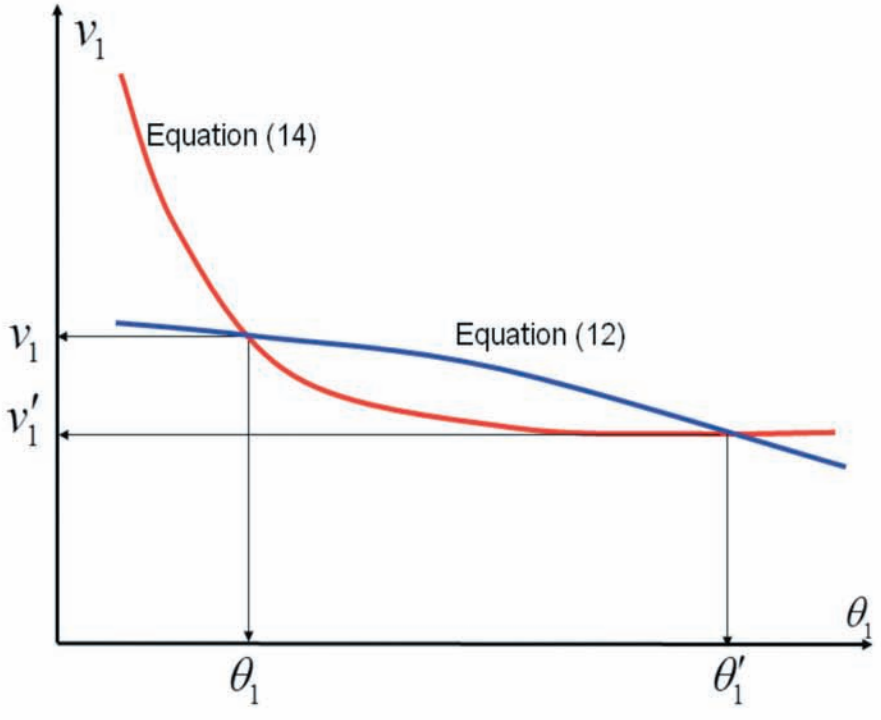

Fig. 3. Graphical solution of two distinct v_1 and θ_1, obtained from common solution of eqs. (12) and (14).

$$\left[\frac{v_o^2}{A^2} - 1 - B\right]^2 = 4B \quad , \tag{28}$$

should be satisfied. Manipulation of this formula leads to:

$$\frac{v_o^2}{A^2} - 1 - B = 2\sqrt{B} \quad , \tag{29}$$

$$\frac{v_o}{A} = \sqrt{B} + 1 \quad . \tag{30}$$

Using eqs. (15) and (16), we find

$$x_c\left(\frac{v_o(a-b)}{2}+1\right)=x_c-v_o t_{i1} \quad , \tag{31}$$

$$-\frac{(a-b)}{2}=\frac{t_{i1}}{x_c} \quad , \tag{32}$$

$$\frac{1}{2}\left(\frac{1}{v_{l1}}-\frac{1}{v_{r1}}\right)=\frac{t_{i1}}{x_c} \quad . \tag{33}$$

Formula (33) defines the condition for which the non-uniqueness fails and the solution is reduced to one root.

At this point, different possibilities are to be considered:

a. **Horizontal refractor case**

As $a=b=1/v_{r1}=1/v_{l1}$.

This means from eq. (16) that $B = 0$ and from eqs. (22) and (23), we find that the zero root solutions correspond to the relations

$$B=1-v_o^2/A^2=0 \ .$$

and

$$A=\mp v_o \ .$$

In that case from formula (21) we find

$$y^2+\left[\frac{v_o^2}{A^2}-1\right]y=0 \ ,$$

and

$$y_1=0 \ ; \quad y_2=0 \ .$$

b. **Dipping refractor case with one solution:**

In that case, condition formula (33) should be satisfied.

c. **Two distinct solutions:**

In that case, the following inequality condition is true:

$$\frac{1}{2}\left(\frac{1}{v_{l1}}-\frac{1}{v_{r1}}\right)\neq\frac{t_{i1}}{x_c}\ .$$

SYNTHETIC DATA APPLICATION

An example of this method is applied to a synthetic data obtained from a near surface model (Fig. 4). A mute is applied to this synthetic shot (Fig. 5a). From Fig. 5b, we can easily obtain the quantities of v_{l1}, v_{r1}, v_0 and t_{i1} as

$$v_o = 1/0.0006657 = 1500 \text{ m/s}, \quad (34)$$

$$v_{r1} = 1/a = 1/0.0004730 = 2115 \text{ m/s}, \quad (35)$$

$$v_{l1} = 1/b = 1/0.0001734 = 5765 \text{ m/s}, \quad (36)$$

$$t_{i1} = c = 0.3077 \text{ s}. \quad (37)$$

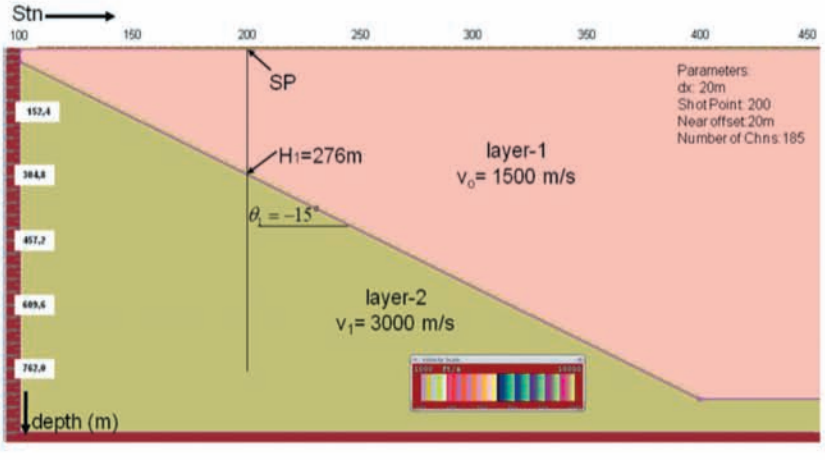

Fig. 4. Near-surface model for synthetic data example, [Spread configurations: Number of channel: 185, Shot Point: 200.5, Stations: 100-450, chn#1 at station 151, chn#185 atstation 335 and Station interval: 20 m].

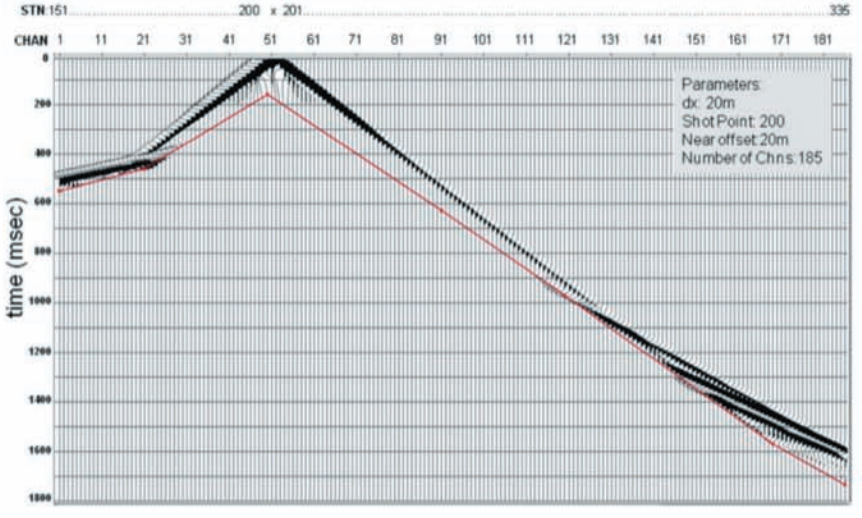

Fig. 5a. Muted version of the synthetic record.

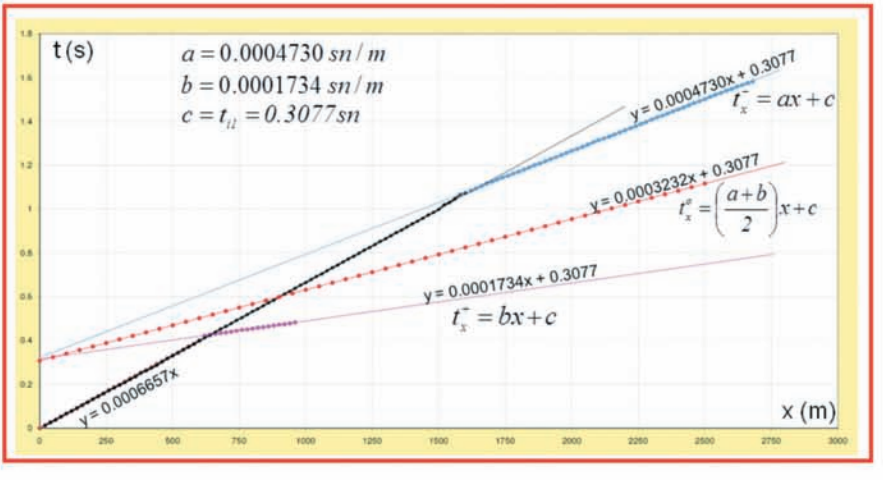

Fig. 5b. Graphical evolution of the values of a, b, c and v_o.

Using either one of eqs. (25a) and (25b) or the intersection points shown in the graphical solution (Fig. 6), the following values are found for θ_1, v_1, H_1 and θ_1', v_1', H_1'.

$\theta_1 = -15^o$ $\qquad$ $\theta_1' = -60.03^o$
$v_1 = 2999.89$ m/s $\qquad$ $v_1' = 1551.43$ m/s
$H_1 = 276.3$ m $\qquad$ $H_1' = 938.1$ m

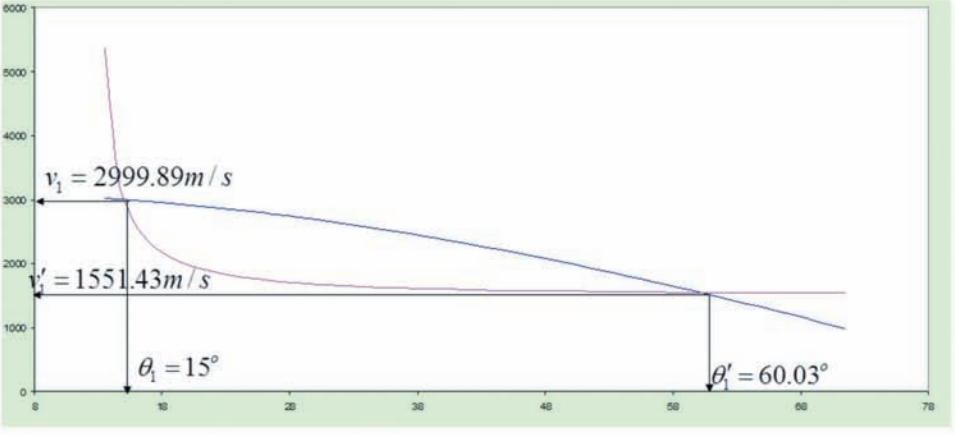

Fig. 6. Graphical solution of v_1 and θ_1 illustrating the existence of the two set of solutions.

Perfect agreement exists between t-x graphics (Fig. 7) of the two models corresponding to two distinct solutions.

Ambiguity is removed, if necessary, taking into account a priory information based on the geological and geophysical background. In this case as we know, in advance, the result which corresponds to the solution obtained by the classical method, our preference goes obviously to this solution. The second solution is to be rejected as it does not seem plausible. The same result is obtained by combining graphical representation of formulas (12) and (14) as shown in Fig. 6.

At this point it may be relevant to calculate the same parameters using classical method for comparison with the results obtained by our method. The most commonly approach to this problem, as we mentioned in the introduction, is the classical intercept method which resolve two unknowns i_1 and θ_1 respectively the angle of incidence and the dip angle of the refractor through two linear eqs. (A-7) and (A-8). We start, then, from the input parameters (34), (35), (36), (37) and using (A-7), (A-8), (12), (26) and (27) we find

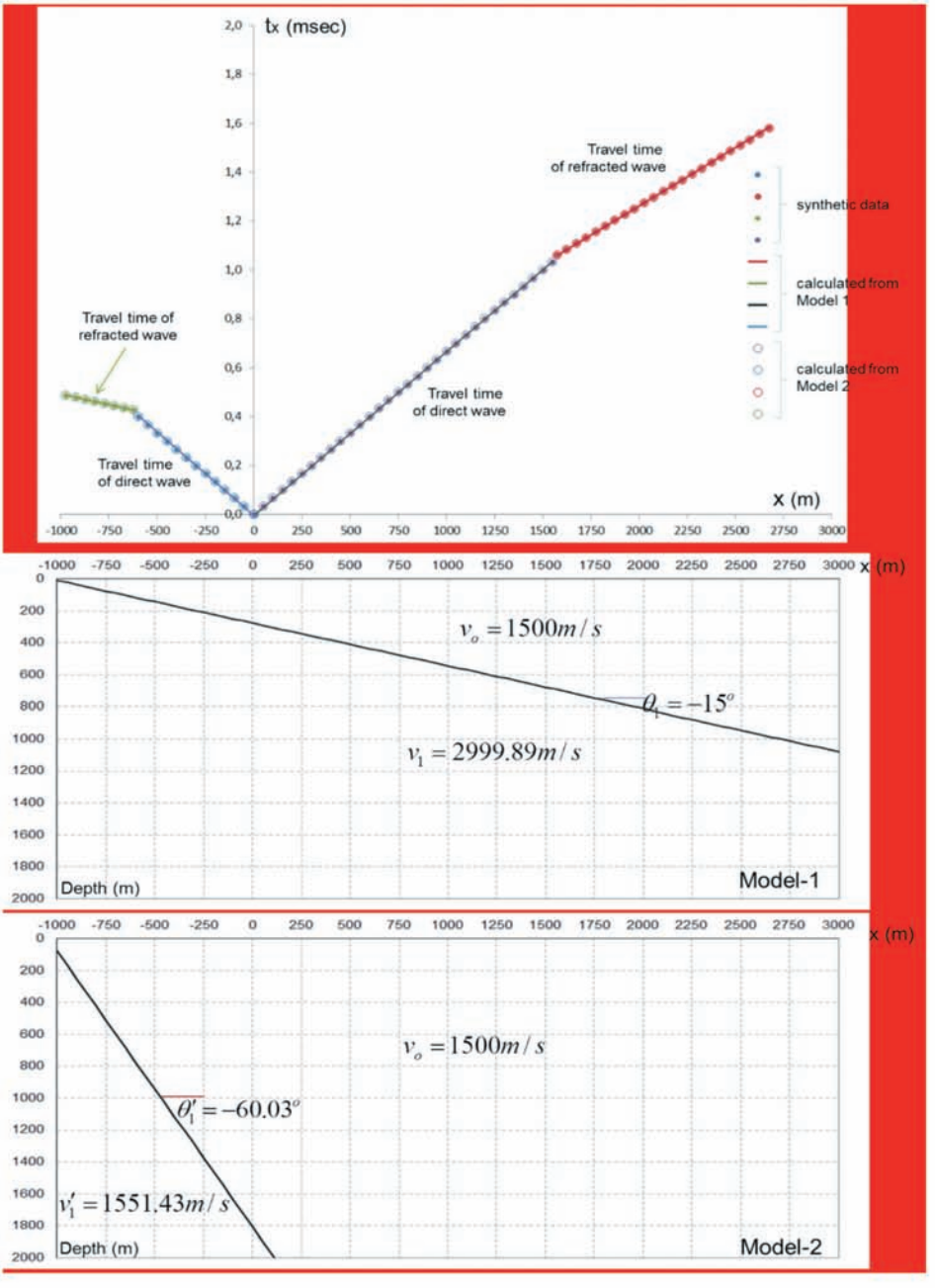

Fig. 7. Comparison of t-x graphics of Model-1 and Model-2

$$i_1 = \frac{1}{2}\left[\arcsin\frac{v_o}{v_{1b}} + \arcsin\frac{v_o}{v_{1a}}\right] = \frac{1}{2}\left[\arcsin\frac{1500}{2115} + \arcsin\frac{1500}{5765}\right],$$

$$i_1 = 30.19^o.$$

$$\theta_1 = \frac{1}{2}\left[\arcsin\frac{v_o}{v_{1a}} - \arcsin\frac{v_o}{v_{1b}}\right] = \frac{1}{2}\left[\arcsin\frac{1500}{2115} - \arcsin\frac{1500}{5765}\right],$$

$$\theta_1 = -15.09^o.$$

$$v_1 = v_o / \sin i_1 = 1500/\sin(15.09) = 2988.82 \text{ m/s}.$$

$$Z_1 = \frac{v_o t_{i1}}{2\cos i_1} = \frac{1500 * 0.3077}{2\cos(30.19^o)},$$

$$Z_1 = 266.81 \text{ m}.$$

$$H_1 = \frac{Z_1}{2\cos\theta_1} = \frac{266.8}{2\cos(-15.09^o)},$$

$$H_1 = 276.28 \text{ m}.$$

Excellent concordance is observed between two sets of values as should be expected.

FIELD DATA APPLICATION

A field data example for a 2-layer case, which is acquired from ARAR Petrol and Gas AS, an oil and gas company in Turkey, is taken from Güreli (2014). Acquisition parameters of the input data are as follows:

number of channels: 204,
far offset: 2170 m,
near offset: 10 m,
shot point: midpoint between station numbers 195 and 196,
group interval: 20 m,
energy source: 4 vibrators,
record length: 5 s,
sampling rate: 2 ms.

Input data that are reduced to the floating datum (Fig. 8a) are picked in the t-x domain (Fig. 8b).

From Figs. 8c and 8d, we can easily obtain the quantities of v_{l1}, v_{r1}, v_o and t_{i1} as

$$v_o = 1/0.0005000 = 2000 \text{ m/s}, \tag{38}$$

$$v_{r1} = 1/a = 1/0.0004107 = 2435 \text{ m/s}, \tag{39}$$

$$v_{l1} = 1/b = 1/0.0003152 = 3173 \text{ m/s}, \tag{40}$$

$$t_{i1} = c = 0.06 \text{ s}. \tag{41}$$

Using either one of formula (25a) and (25b) or the intersection points shown in the graphical solution (Fig. 8e), the following values are found for θ_1, v_1, H_1 and θ_1', v_1', H_1'.

$\theta_1 = 8.07^o$ $\theta_1' = 42.87^o$

$v_1 = 2728.00$ m/s $v_1' = 2019.27$ m/s

$H_1 = 88.22$ m $H_1' = 435.33$ m

Perfect coincidence of the t-x graphics (Fig. 8f) of the two models corresponding to two distinct solutions can be observed.

Application of the intercept method to the same field data yields

$$i_1 = \frac{1}{2}\left[\arcsin\frac{v_o}{v_{1b}} + \arcsin\frac{v_o}{v_{1a}}\right] = \frac{1}{2}\left[\arcsin\frac{2000}{2435} + \arcsin\frac{2000}{3173}\right],$$

$$i_1 = 47.15^o.$$

$$\theta_1 = \frac{1}{2}\left[\arcsin\frac{v_o}{v_{1a}} - \arcsin\frac{v_o}{v_{1b}}\right] = \frac{1}{2}\left[\arcsin\frac{2000}{2435} - \arcsin\frac{2000}{3173}\right],$$

$$\theta_1 = 8.07^o.$$

$$v_1 = v_o / \sin i_1 = 2000 / \sin(8.07^o) = 2727.89 \text{ m/s} ,$$

$$Z_1 = \frac{v_o t_{i1}}{2\cos i_1} = \frac{2000 * 0.06}{2\cos(47.15^o)} ,$$

$$Z_1 = 88.23 \text{ m} .$$

$$H_1 = \frac{Z_1}{2\cos\theta_1} = \frac{88.2}{2\cos(8.07^o)} ,$$

$$H_1 = 89.11 \text{ m} .$$

Equivalence of the intercept solution with the first set of values obtained by our method is apparent. But the second set of solutions does not appear with the intercept method.

CONCLUSIONS

In this paper we propose, in addition to the existing ones, a new method of the refraction prospecting which has not been reported previously. We recognize that this calculation of the refraction statics, though the method does not imply any approximation and it is perfectly accommodating with the computer processing, has no noticeable advantage with respect to the others.

Through this new approach, we show the existence of a second degree solution of the refraction problem and as a subsequent result the perspective of the distinct theoretical solutions that honor the same data. Generally speaking the modeling related to the second solution can be hardly encountered in geological medium. But in physical space the both solutions, free of the geological constraints, can be easily conceivable. In that sense interest of the second solution case appears to be theoretical rather than prospective and investigation of this problem is not related only to the seismic refraction prospecting.

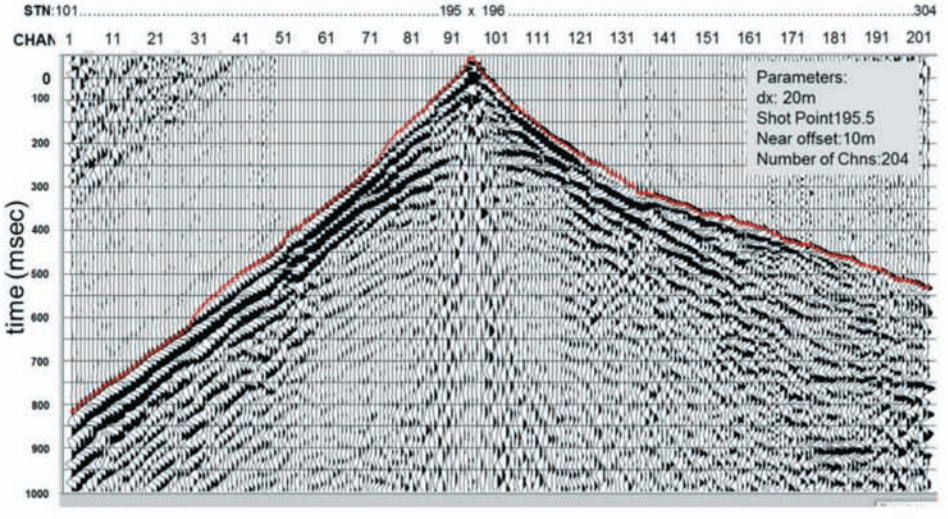

Fig. 8a. Gain (t**0.2) and AGC 1000 ms applied real data reduced to the floating datum, [Spread configurations: Number of channel: 204, Shot Point: 195.5, Stations: 101-304, chn#1 at station 101, chn#204 at station 304 and Station interval: 20m, Near offset: 10 m].

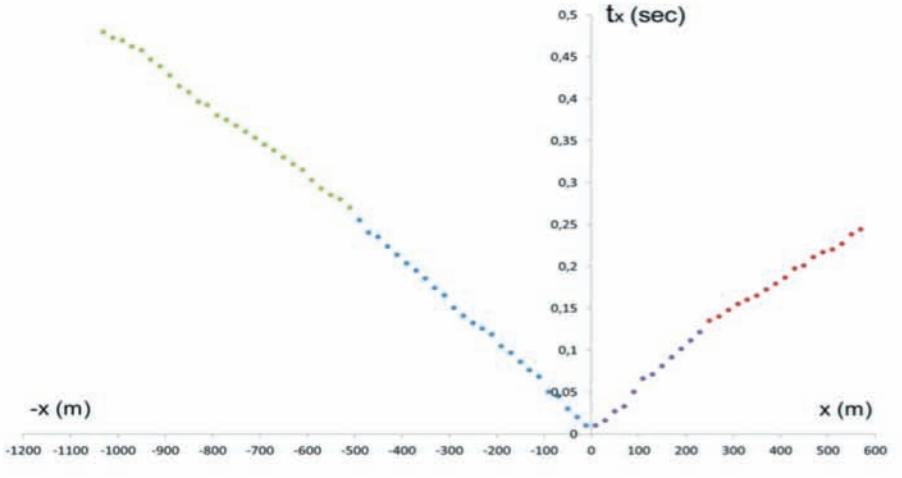

Fig. 8b. t-x graphic of Fig. 8a.

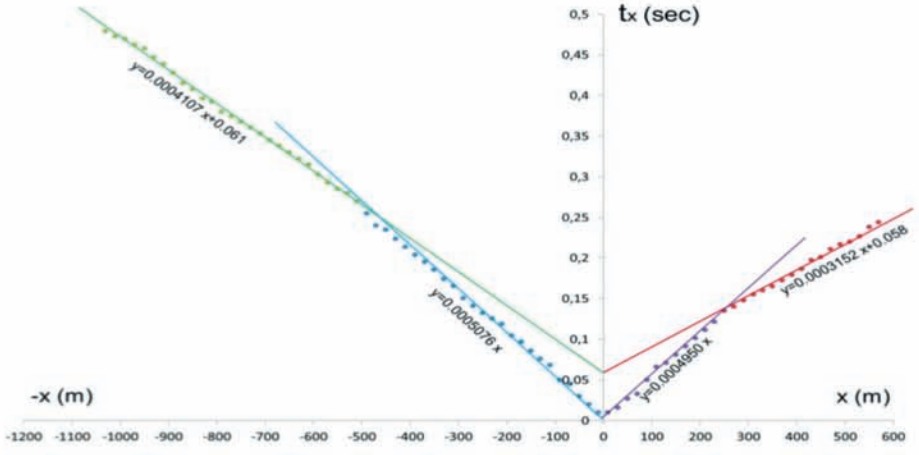

Fig. 8c. Evaluation of t-x graphic of Fig. 8b.

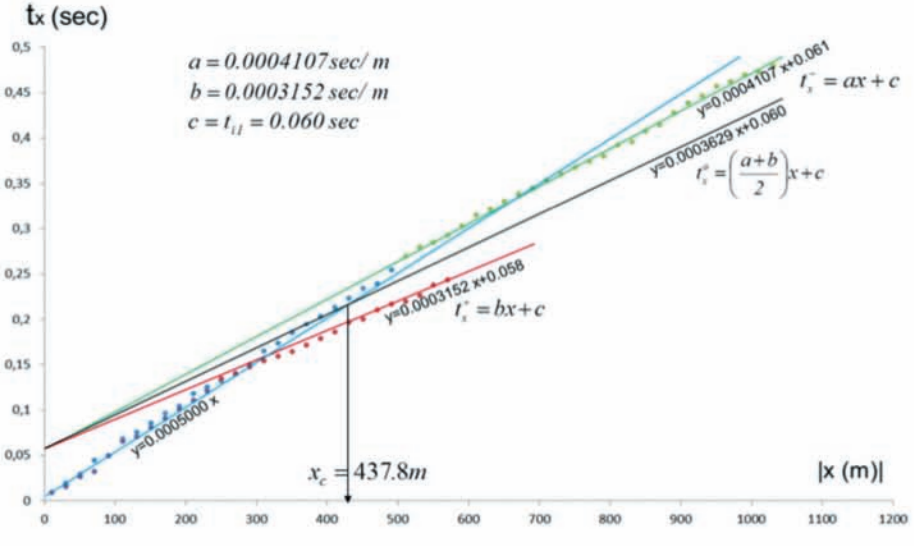

Fig. 8d. Evaluation of t-x graphic with absolute of Figure 8c.

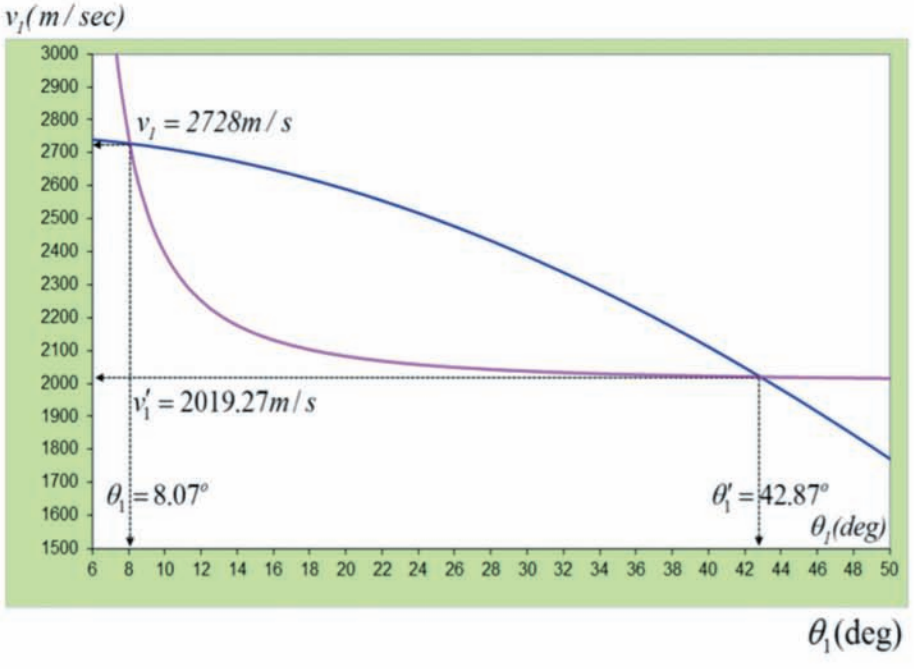

Fig. 8e. Graphical solution of v_1 and θ_1 illustrating the existence of the two set of solutions for real data.

It should be noted that, considering the example given in this paper, the difference between the first medium velocity and refractor velocity is relatively poor to obtain an acceptable result without applying a special acquisition and processing treatment. However the proposed approach in this paper represent the very complete solution related to this problem and justly we believe that it may deserve a place among the plethora of the various existing refraction methods.

ACKNOWLEDGEMENT

We are grateful to ARAR Petrol and Gas AUP AS. (Turkey) for providing the 2D seismic field data used in this paper.

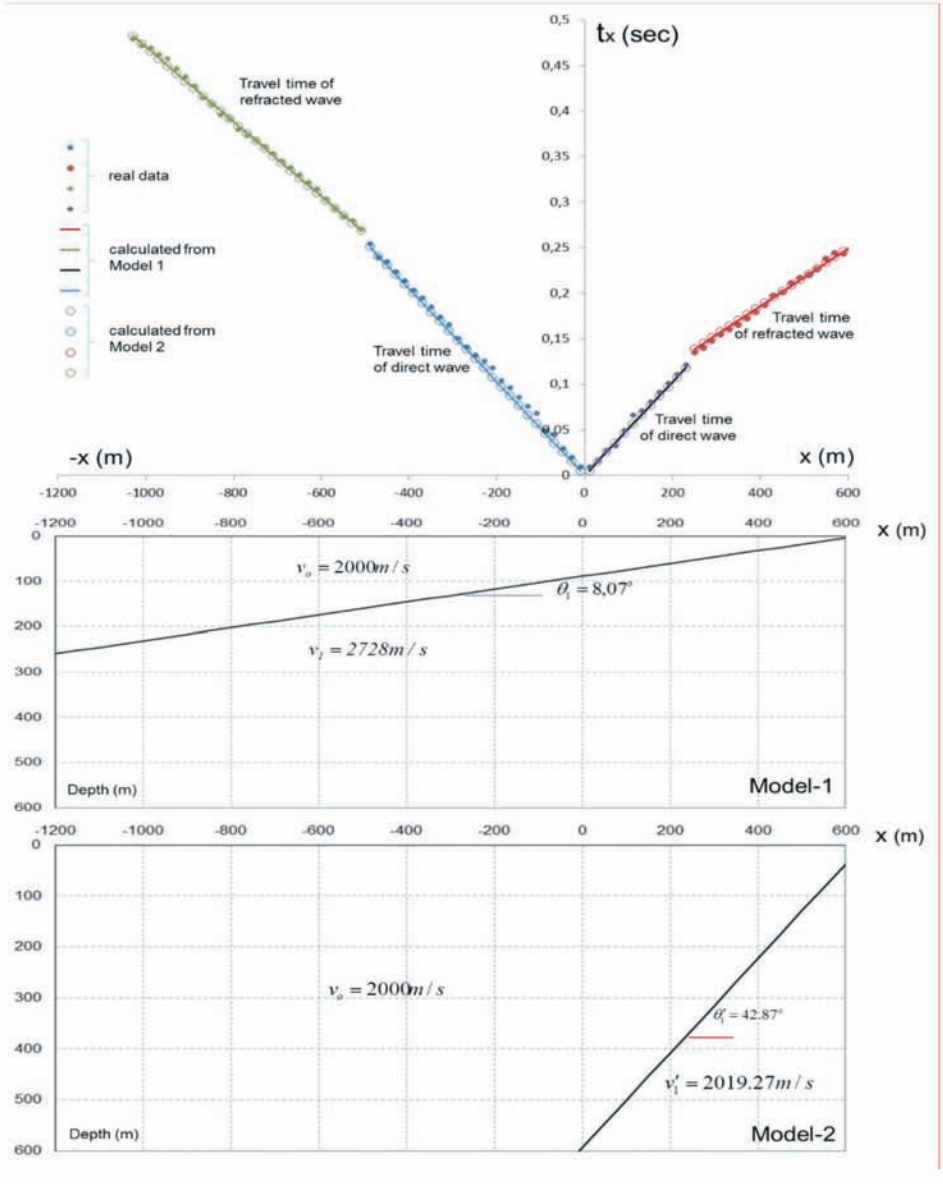

Fig. 8f. The comparison of the first arrival times re-calculated starting from Model 1 and Model 2 with first break times of the real data.

REFERENCES

Barry, K.M., 1967. Delay time and its application to refraction profile interpretation. In: Musgrave, A.W. (Ed.), Seismic Refraction Prospecting: 348–361. SEG, Tulsa, OK.

Barthelmes, A.J., 1946. Application of continuous profiling to refraction shooting. Geophysics, 11: 24–42.

Chang, X., Liu, Y., Wang, H., Li. F., Chen, J., 2002. 3-D tomographic static correction. Geophysics, 67: 1275-1285.

Docherty, P., 1992. Solving for the thickness and velocity of the weathering layer using 2D refraction tomography. Geophysics, 97: 1307-1318.

Gardner, L.W., 1939. An areal plan of mapping subsurface structure by refraction shooting. Geophysics, 4: 247–259.

Güreli, O., 2014. Determination of dips and depths of near surface layers by Radon transform. Pure Appl. Geophys., 171: 1805-1827.

Hagedoorn, J.G., 1959. The Plus-Minus method of interpreting seismic refraction sections. Geophys. Prosp., 7: 158-182.

Hales, F.W., 1958. An accurate graphical method for interpreting seismic refraction lines. Geophys. Prosp., 6, 285–314.

Mota, L., 1954. Determination of dips and depths of geological layers by seismic refraction method. Geophysics, 19: 242-254.

Shtivelman, V., 1996. Kinematic inversion of first arrivals of refracted waves - A combined approach. Geophysics, 61: 509-519.

Tarrant, L.H., 1956. A rapid method of determining the form of a seismic refractor from line rofile results. Geophys. Prosp., 4: 131–139.

Telford, W.M., Geldart, L.P. and Sherriff, R.E., 1990. Applied Geophysics, 2nd Ed. Cambridge University Press, Cambridge, 770 pp.

Thornburgh, H.R., 1930. Wave front diagrams in seismic interpretation. AAPG Bull., 14: 185–200.

White, D.J., 1989. Two-dimensional seismic refraction tomography, Geophys. J. Internat., 97: 223-245.

Zhang, J. and Toksöz, M.N., 1998. Nonlinear refraction traveltime tomography. Geophysics, 63: 1726-1737.

APPENDIX

CASE OF RECIPROCAL TIME GEOMETRY

From Fig. (A-1), we can write for $+x$ direction

$$t_x^+ = \frac{OA}{v_o} + \frac{AB}{v_1} + \frac{BC}{v_o} = \frac{Z_1 + z_1'}{v_o \cos i_1} + \frac{x \cos\theta_1}{v_1} - \frac{(Z_1 + z_1')}{v_1} \tan i_1. \qquad \text{(A-1)}$$

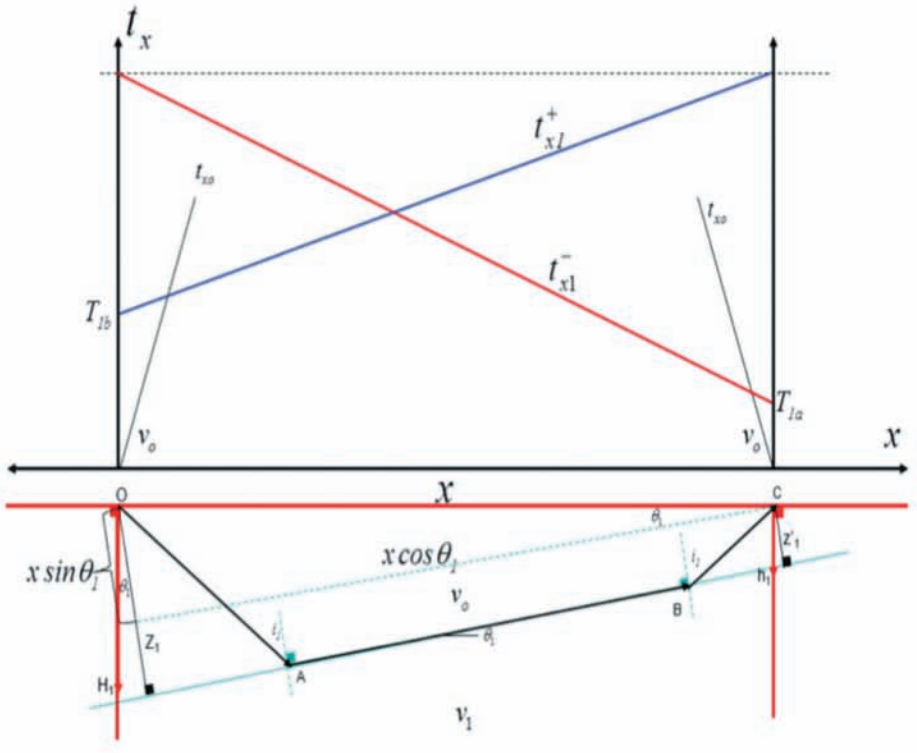

Fig. A-1. Refraction along the top of a layer with velocity v_1 overlain by a layer with a lower velocity v_o.

Putting $sin\, i_1 = \dfrac{v_o}{v_1}$ and after same manipulations and simplifications, we obtain:

$$t_x^+ = \frac{x}{v_o} sin(i_1 - \theta_1) + \frac{2Z_1}{v_o} cos\, i_1. \qquad \text{(A-2)}$$

where

v_o : the first layer velocity,

θ_1 : the dip measured from the horizontal for the first interface,

i_1 : critical angle for the first interface,

Z_1 : the perpendicular depth of the refractor at the shot point O (see Fig A-1).

In a similar way we find for the $-x$ direction

$$t_x^- = \frac{x}{v_o} sin(i_1 + \theta_1) + \frac{2z_1'}{v_o} cos\, i_1. \qquad \text{(A-3)}$$

where

z_1': the perpendicular depth of the refractor at the shot point C (see Fig. A-1).

Taking apparent velocities as:

$$v_{1a} = \frac{v_o}{sin(i_1 + \theta_1)} \quad , \qquad v_{1b} = \frac{v_o}{sin(i_1 - \theta_1)} \quad , \qquad \text{(A-4)}$$

and intercept times as:

$$T_{1b} = \frac{2Z_1}{v_o} cos\, i_1 = \frac{2Z_1}{v_o v_1} \sqrt{v_1^2 - v_o^2}\,, \qquad \text{(A-5)}$$

$$T_{1a} = \frac{2z_1'}{v_o} cos\, i_1 = \frac{2z_1'}{v_o v_1} \sqrt{v_1^2 - v_o^2}\,. \qquad \text{(A-6)}$$

we find

$$i_1 - \theta_1 = arcsin \frac{v_o}{v_{1b}},$$

$$i_1 + \theta_1 = arcsin \frac{v_o}{v_{1a}},$$

$$i_1 = \frac{1}{2}\left[arcsin \frac{v_o}{v_{1b}} + arcsin \frac{v_o}{v_{1a}} \right]. \qquad \text{(A-7)}$$

$$\theta_1 = \frac{1}{2}\left[arcsin \frac{v_o}{v_{1a}} - arcsin \frac{v_o}{v_{1b}} \right]. \qquad \text{(A-8)}$$

$$t_x^+ = \frac{x}{v_{1b}} + T_{1b} = \frac{x}{v_{1b}} + \frac{2Z_1}{v_o v_1} \sqrt{v_1^2 - v_o^2}\,. \qquad \text{(A-9)}$$

$$t_x^- = \frac{x}{v_{1a}} + T_{1a} = \frac{x}{v_{1a}} + \frac{2z_1'}{v_o v_1} \sqrt{v_1^2 - v_o^2}\,. \qquad \text{(A-10)}$$

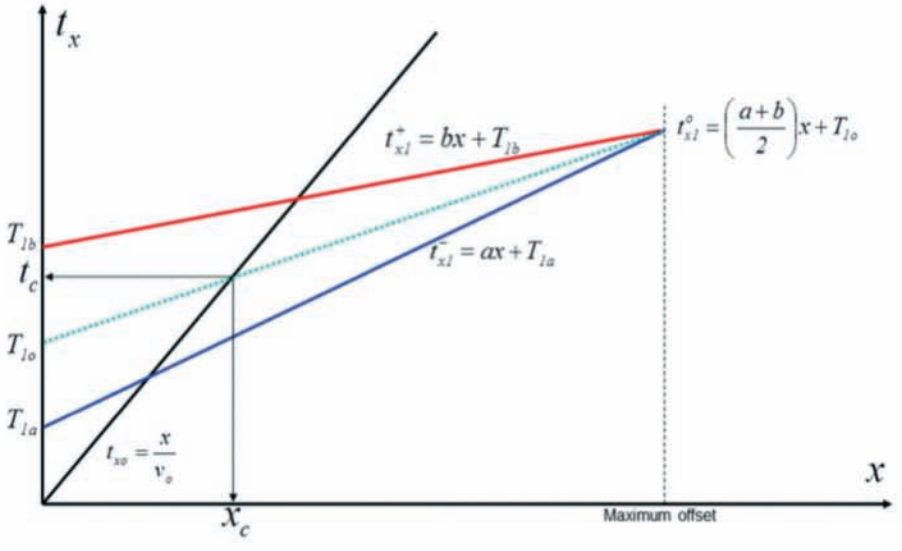

Fig. A-2. Graphical evolution of the values of a, b, T_{1a}, T_{1b}, T_{1o} and v_o.

These two last equations represent two equations (Fig. A-2), where

$$v_{1b} = \frac{v_o}{sin(i_1 - \theta_1)}. \tag{A-11}$$

$$v_{1a} = \frac{v_o}{sin(i_1 + \theta_1)}. \tag{A-12}$$

The arithmetic mean of these two equations

$$t^o_x = \frac{t^+_x + t^-_x}{2} = \frac{x}{2}\left(\frac{1}{v_{1b}} + \frac{1}{v_{1a}}\right) + \frac{\left(T_{1a} + T_{1b}\right)}{2},$$

$$t^o_x = \frac{x}{2}\left(\frac{1}{v_{1b}} + \frac{1}{v_{1a}}\right) + T_{1o}, \tag{A-13}$$

where $T_{1o} = \frac{\left(T_{1a} + T_{1b}\right)}{2}$.

If x_c is the intersection point of the mean line with the line $\frac{x}{v_o}$, x_c is found to be as:

$$x_c = \frac{-T_{1o}}{\frac{1}{2}\left(\frac{1}{v_{1b}} + \frac{1}{v_{1a}}\right) + \frac{1}{v_o}}. \qquad \text{(A-14)}$$

Substituting (A-11) and (A-12) into (A-14) we obtain

$$\frac{x_c}{v_o} \sin i_1 \cos\theta_1 + T_{1o} = \frac{x_c}{v_o}. \qquad \text{(A-15)}$$

Using Snell law $\left(\sin i_1 = \frac{v_o}{v_1}\right)$, (A-15) becomes

$$\frac{v_1}{x_c \cos\theta_1} = \frac{v_o}{x_c - v_o T_{1o}},$$

and we find

$$v_1 = \frac{v_o x_c \cos\theta_1}{x_c - v_o T_{1o}}. \qquad \text{(A-16)}$$

On the other hand if we calculate

$$a - b = \frac{1}{v_{1a}} - \frac{1}{v_{1b}} = \frac{\sin(i_1 + \theta_1)}{v_o} - \frac{\sin(i_1 - \theta_1)}{v_o},$$

we find for v_1

$$v_1 = \frac{2v_o \sin\theta_1}{\left[4\sin^2\theta_1 - v_o^2\left(\frac{1}{v_{1b}} - \frac{1}{v_{1a}}\right)^2\right]^{1/2}}. \qquad \text{(A-17)}$$

As (A-16) and (A-17) are identical to (12) and (14) the rest of the calculation is justiciable of the same procedure as explained in the main text and we arrive to the same result.